Available online at www.sciencedirect.com
ScienceDirect
Journal of Molecular Graphics and Modelling 26 (2007) 145–153
Journal of Molecular Graphics and Modelling
www.elsevier.com/locate/JMGM

Development of CoMFA models of affinity and selectivity to angiotensin II type-1 and type-2 receptors

Christian Sköld, Anders Karlén *

Division of Organic Pharmaceutical Chemistry, Department of Medicinal Chemistry, BMC, Uppsala University, Sweden

Received 24 May 2006; received in revised form 26 September 2006; accepted 20 October 2006
Available online 26 October 2006

Abstract

The renin-angiotensin system (RAS) is of major importance in cardiovascular and renal regulation and has been an attractive target in drug discovery for a long time. The main receptors involved in the RAS are the Angiotensin type-1 (AT_1) and type-2 (AT_2) receptors, which are both activated by the endogenous octapeptide angiotensin II (AngII). This study describes the development of 3D-QSAR models for AT_1 and AT_2 receptor affinity and AT_1/AT_2 receptor selectivity using CoMFA. A data set of 244 compounds, based on the triazolinone and quinazolinone structural classes was compiled from the literature. Before CoMFA could be performed, an alignment rule for the two structural classes was defined using the pharmacophore-searching program DISCOtech. Models were validated using a test set obtained by dividing the data set into a training set and test set using hierarchical clustering, based on the CoMFA fields, AT_1-, AT_2-receptor affinities, and AT_1/AT_2 selectivity values. Predictive models with good statistics could be developed both for AT_1 and AT_2 receptor affinity as well as selectivity towards these receptors.

Keywords: Angiotensin; AT_1; AT_2; Selectivity; CoMFA; 3D-QSAR; DISCOtech; Training set selection

1. Introduction

The renin-angiotensin system (RAS) is of major importance in cardiovascular and renal regulation and has been an attractive target in drug discovery for a long time. The main receptors involved in the RAS are the Angiotensin type-1 (AT_1) and type-2 (AT_2) receptors, both activated by the endogenous octapeptide angiotensin II (AngII) [1]. The AT_1 receptor is well studied and is mainly known for regulating blood pressure and there are a number of AT_1 receptor selective antagonists on the market today used for treating hypertension. The AT_2 receptor is less well-understood and interestingly the stimulation of the AT_1 and AT_2 receptors has, in many cases, direct opposing effects [2]. The AT_2 receptor has been shown to be involved in many different processes, such as cell differentiation, tissue repair [3], alkaline secretion in the rat duodenum [4], and in cardioprotective effects [5]. There is now a belief that development of a selective AT_2 receptor agonist could be important for therapeutic purposes in the areas of hypertension and cardiac remodeling [6,7].

The first selective AT_1 receptor antagonist losartan was launched by Merck in 1994 and this compound was soon followed by a series of compounds known as the ''sartans'' drug family. Studies in the 1990s showed that the administration of AT_1-selective AngII antagonists results in a renin-mediated increase in the plasma levels of AngII and a stimulation of AT_2 receptors with an unknown long-term effect. To avoid this unwanted effect, balanced AT_1/AT_2 receptor antagonists capable of equally blocking both receptor subtypes were developed. It was speculated that these compounds would be useful as pharmacological tools and could prove valuable as therapeutic agents. Several series of compounds were synthesized by, for example, modifying the AT_1 selective antagonists to enhance the AT_2 affinity but no compounds with this profile have yet reached the market [8,9].

Our long-term objective is to develop non-peptide ligands that interact with the AT_2 receptor. It therefore seemed appealing to build on the structure–activity data generated for the balanced AT_1 and AT_2 receptor and build 3D-QSAR models that could be used for the further design of selective AT_2 receptor ligands. Many 3D-QSAR studies have previously been published for the AT_1 receptor [10–15] but only a few for the AT_2 receptor [11,12]. The aim of our study was therefore to: (a)

* Corresponding author. Tel.: +46 18 471 4293; fax: +46 18 471 4474.
E-mail address: anders.karlen@orgfarm.uu.se (A. Karlén).

1093-3263/$ – see front matter © 2006 Elsevier Inc. All rights reserved.
doi:10.1016/j.jmgm.2006.10.004

identify a ''high-quality'' data set of balanced AT_1 and AT_2 receptor ligands measured by a single protocol, (b) define a conformation and alignment for the ligands, based on pharmacophore searching using DISCOtech [16] and (c) build robust 3D-QSAR models using comparative molecular field analysis (CoMFA) [17] that can be used for predicting AT_1 and AT_2 receptor affinity and AT_1/AT_2 selectivity.

2. Methods

2.1. Data set selection

The data set used in this study was derived from a series of ligands with both AT_1 and AT_2 receptor affinities and comprise 182 triazolinones (cf. **1**) and 62 quinazolinones (cf. **2**) [18–25]. We reviewed the literature and selected only those publications where the binding affinity of these compounds was measured by a single protocol and were derived from the same laboratory. The affinities ranged from 0.04 nM to 1.3 μM and 0.06 nM to 29 μM for the AT_1 and AT_2 receptors, respectively. Analogs with unknown chirality, unique scaffold features, or with limiting values for the IC_{50} (e.g. >10 μM) were not considered in the modeling. Since a functional correlate for the AT_2 receptor was missing at the time when these studies were performed, only in vitro AT_1 and AT_2 receptor binding affinity was reported. It should be mentioned that this is still essentially the case and the functional activity of only a few AT_2 receptor ligands are known.

2.2. Preparation for data set alignment

To align the compounds in the data set, the pharmacophore searching program DISCOtech was used. For this analysis, compounds **1** and **2** (Fig. 1) were selected as representative compounds from each structural class and a conformational analysis of these compounds was performed using MacroModel 7.1 [26]. The setup was 5000 steps per rotational bond using the Systematic Unbound Multiple Minimum search method [27] and 500 minimization steps using Truncated Newton Conjugate Gradient [28] (TNCG) with derivative convergence set to 0.05 kJ mol^{-1} $Å^{-1}$ and the MMFF94s force field. The General Born Solvent Accessible (GB/SA) surface area method for water developed by Still et al. [29] was used in the calculations. All heavy atoms were compared to identify unique conformations. Amide bonds were locked in the trans configuration. All conformations within 5 kcal/mol from the lowest identified energy minimum were kept (resulting in 9992 and 31169 conformations for **1** and **2**, respectively). Because of a limit of 300 conformations per molecule that can be used in the following DISCOtech analysis, a reduction in the number of conformations was required. This was performed in two different consecutive steps. First, all conformations were reminimized with a maximum of 500 steps using the TNCG method and the convergence was set to 0.001 kJ mol^{-1} $Å^{-1}$. In this minimization step only a reduced set of atoms were compared (see supplementary material) to identify unique conformations. These atoms were selected as they either correspond to features used in DISCOtech or to key atoms in the molecule. This generates a reduced set of conformations that are diverse with regard to important pharmacophore features that will be used in the DISCOtech search. In a second step, the rigidified macrocyclic analogue **3** (Fig. 1) was used to reduce the number of possible conformations of the acylsulfonamide moiety in **1** and **2**. It was shown by de Laszlo et al. that the binding affinity to the AT_1 and AT_2 receptors of macrocyclic quinazolinones analogues including **3** was not substantially reduced as compared to structurally similar linear analogues [15]. Thus, even though **3** has lower AT_1 and AT_2 receptor affinity as compared to **1** and **2**, it should be relevant to compare their conformational properties since the difference in affinity is not likely due to the cyclization per se but rather to other structural differences in the molecules. Conformations within 5 kcal/mol of the lowest identified energy minimum of **3** were generated according to the procedure described above. The improper torsion angle N-C-C-S (shown in Fig. 1 with

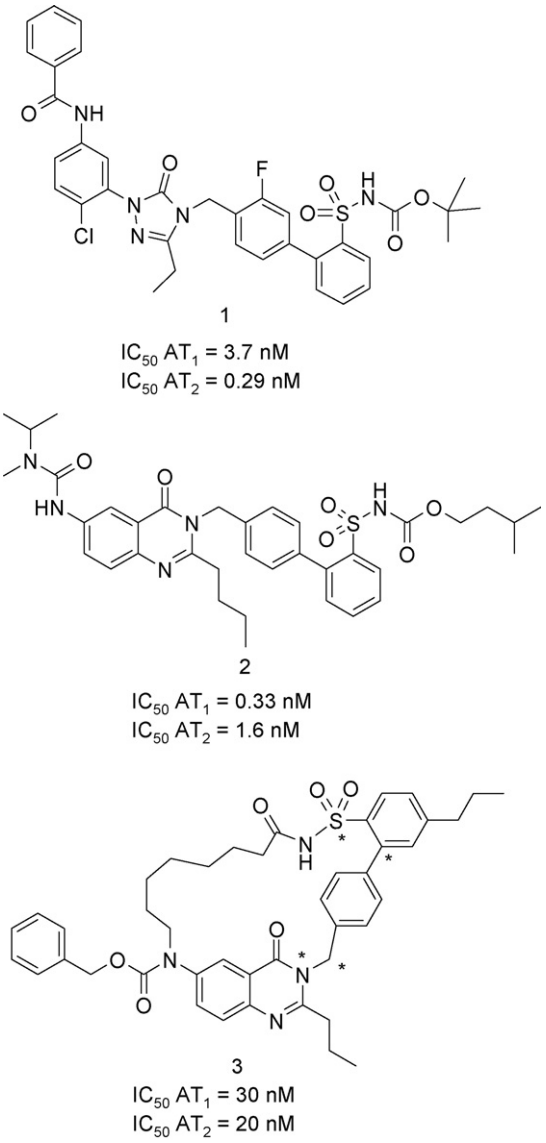

Fig. 1. Reference structures used in the modeling.

asterisks) that describes the direction of the sulfonamide moiety as compared to the heteroaromatic scaffold was used as the geometric filter. This torsion angle only varies between $0 \pm 90^{\circ}$ in the found conformations of **3**. When measuring the corresponding torsion angle in the conformations of **1** and **2** and applying this range as a filter, combined with an increased atom pair distance criterion of 1.5 Å between the reduced set of atoms when defining unique conformations (BatchMin command CRMS), the number of conformations was reduced to 132 for **1** and 471 for **2**. The number of conformations of **2** was further reduced by selecting only the 300 conformations with the lowest energy, which corresponds to conformations within 4.16 kcal/mol from the lowest found minimum.

2.3. Data set alignment using DISCOtech

To obtain reasonable conformations and a reasonable superimposition that would ideally reflect the bioactive conformation of the analogues, the DISCOtech program was used to align possible pharmacophore features in **1** and **2**. 132 conformations of **1** and 300 conformations of **2** were used in the DISCOtech analysis. DISCOtech first assigns pharmacophore elements such as hydrogen bond donor atoms, hydrogen bond acceptor atoms, charged centers, hydrophobic groups, centers of mass of hydrophobic rings and the most likely location of binding sites in the receptor macromolecule to the molecules. The hydrophobic feature in **2** originating from the butyl group connected to the quinazolinone moiety was removed since the corresponding shorter ethyl group in **1** is not considered to be a hydrophobic feature by DISCOtech. If this feature is kept, DISCOtech will try to map it to other hydrophobic elements in **1**, resulting in models with improbable alignments (i.e. the heterocyclic rings not aligned). The ''features by class'' options in DISCOtech was used and the number of pharmacophore features required in each class was set to more than two acceptor atoms, more than two hydrophobic features, one negative center and one positive center. The distance tolerance between the pharmacophore features in the overlaid structures was set to 0.25 Å, increasing up to 0.5 Å if no model was found using the lower tolerance setting (step size 0.25 Å). Compound **1** was used as the reference molecule in all models.

2.4. Comparative molecular field analysis (CoMFA)

CoMFA is a 3D-QSAR method deriving interaction energies from a probe atom at grid points surrounding the compounds. These interaction energies are correlated with a response, often affinity, using projection to latent structures (PLS). Given that a correlation exists and if a good alignment of the data set compounds has been made, the effects on the response from different structural features in the data set can each be identified. The alignment model including both compounds generated in DISCOtech was oriented in Sybyl [30] using the command Orient_best_view. The compounds used for CoMFA modeling were built using either structure **1** or **2** from the DISCOtech model as templates. Since many structural features were not included in the pharmacophore model several rules had to be defined when building these compounds. For example, the alkyl chains on the heterocyclic moieties were built in an extended conformation. Also, care was taken to build the molecules as consistently as possible in cases where alternative rotamers could influence the positioning of differently sized groups.

To fix possible non-optimal geometries obtained during the building, each structure was minimized. First, to prevent the structures from moving away from the alignment, an aggregate was defined for each structure which included the heavy atoms in the triazolinone or quinazolinone rings, the biphenyl moiety, and the sulfonamide group. Each molecule was minimized to convergence in Sybyl using the MMFF94s force field with MMFF charges and a dielectric constant of 78, otherwise default settings were used. After minimization, AM1 [31] charges were calculated and applied using the MOPAC module in Sybyl. The use of AM1 charges in CoMFA has sometimes shown improved results [32]. The CoMFA modeling was performed in Sybyl with standard settings and with a region defined from all 244 compounds. Affinities and selectivity ratio for the compounds were transformed into negative logarithms, pAT1, pAT2 and pSel (pSel = pAT1 − pAT2). High values in the transformed responses thus correspond to high affinity, or in the case of pSel, high AT_1 receptor selectivity.

2.5. Selection of training and test set

In order to produce a training set including as much information as possible, while still allowing the exclusion of compounds for a validation set, a diverse subset of compounds from the original 244 structures were assigned to the training set. The ratio of compounds for the training and test set was chosen to 50%. The selection was based on hierarchical clustering using the CoMFA field values, pAT1, pAT2 and pSel. Column filtering was set to 1 kcal/mol and CoMFA standard scaling was used. Using the hierarchical clustering module in Sybyl, 122 clusters were derived from the data set. One compound from each cluster was arbitrarily selected for the training set and the other for the test set. The distribution of pAT1 and pAT2 values for the training set and test set, respectively, are shown in Fig. 2.

2.6. Projection to latent structures (PLS) analysis

CoMFA field values for the training set were correlated with affinities and selectivity using PLS. The optimum number of components to use was determined by leave-20%-out cross-validation using a maximum of 10 principal components for each response at a time. The suggested number of components for pAT1, pAT2 and pSel was 4, 3, and 5, respectively. This also coincided with the first occurrence of a minimum in the standard error of prediction for the responses. Final models were derived using the suggested number of components. Bootstrapping (100 runs) was used to evaluate the robustness of the models [33] and the risk of chance correlation was assessed using y-randomization (100 runs). The protocol used for

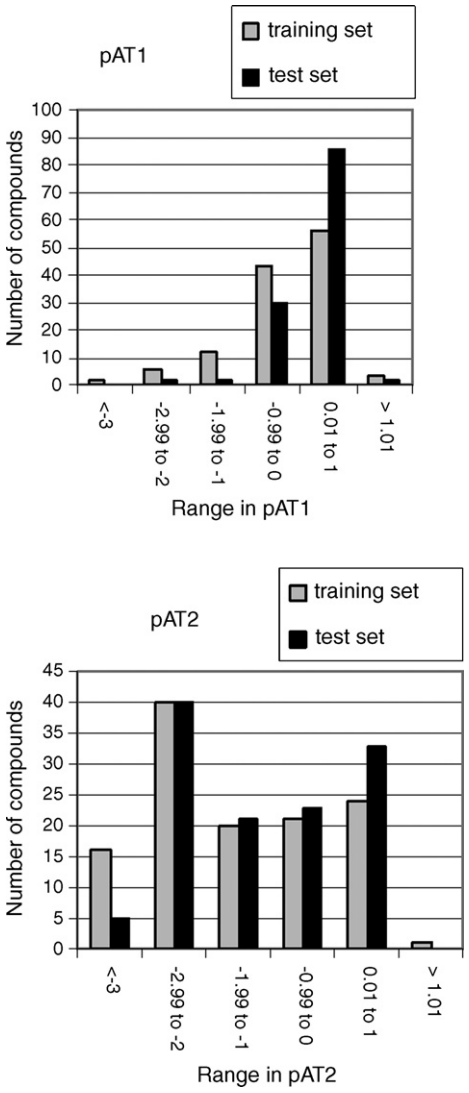

Fig. 2. Distribution of pAT1 and pAT2 values for the training and test set.

y-randomization is identical to that described by Peterson et al. [34].

The responses were predicted for the compounds in the test set and SDEP (standard deviation of error of predictions) and R^2_{pred} were calculated for each response according to the following equations:

$$R^2_{\text{pred}} = 1 - \frac{\sum (y_{\text{pred}} - y_{\text{obs}})^2}{\sum (y_{\text{obs}} - \bar{y}_{\text{obs}})^2} \quad (1)$$

$$\text{SDEP} = \sqrt{\frac{\sum (y_{\text{pred}} - y_{\text{obs}})^2}{n}} \quad (2)$$

where $\bar{y}_{\text{obs}}$ is the mean of the observed training set values and n is the number of compounds in the test set ($n = 122$).

3. Results and discussion

This study describes the development of 3D-QSAR models for AT_1 and AT_2 receptor affinity and AT_1/AT_2 receptor selectivity using CoMFA. First, a putative pharmacophore conformation was derived using DISCOtech, which was later used for aligning the molecules in the data set. In any study, the derivation of a training and test set has a large effect on model predictivity. In this case, data set selection was accomplished using hierarchical clustering, based on CoMFA fields, receptor affinities, and receptor selectivity. The possible merits of this approach are also discussed. Finally, CoMFA models are derived using the complete data set and the contour plots are evaluated.

3.1. DISCOtech analysis

The pharmacophore searching program DISCOtech was used to define an alignment rule for compounds **1** and **2**. DISCOtech derived 3512 possible pharmacophore models. The reason for the large number of models is mainly due to the structural and conformational similarity of the two input structures, which leads to families of very similar models. The highest number of common features (donor sites, acceptor atoms, etc.) was 15 and this was found in the vast majority of models. The DISCOtech score of the models ranged from 6.31 to 9.38. To sort out models with a good alignment and a high structural overlap the common volume of each model was calculated. The underlying rational for this approach is that, given a high score, a model with a relative small volume is likely to have a large structural overlap and thus a good overall alignment. The model with the smallest volume, which also has a high score (8.38), is shown in Fig. 3. In this model most of the structural features are aligned in an intuitive way. One difference between the conformations of the two molecules can be found near the aryl amide/aryl urea moiety where the CONH group points in opposite directions in compounds **1** and **2**, respectively. Furthermore, when the torsion angle of the acylsulfonamide moiety in compounds **1** and **2** were compared to crystal structures of benzene sulfonamides in the Cambridge Structural Database [35], they did not adopt identical values. Despite these shortcomings, the conformations adopted by the two molecules in this model were used as templates when building the remaining compounds of the data set. This model also provided the alignment rule in the CoMFA study.

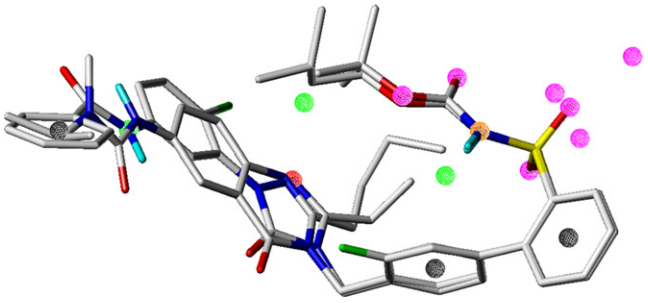

Fig. 3. Alignment of **1** and **2**, obtained using DISCOtech. Spheres indicate pharmacophore features common to the two structures. Color codes: gray = -hydrophobic, pink = hydrogen bond acceptor (ligand) or hydrogen bond donor (receptor site), green = hydrogen bond donor (ligand) or hydrogen bond acceptor (receptor site), red = positive center, orange = negative center.

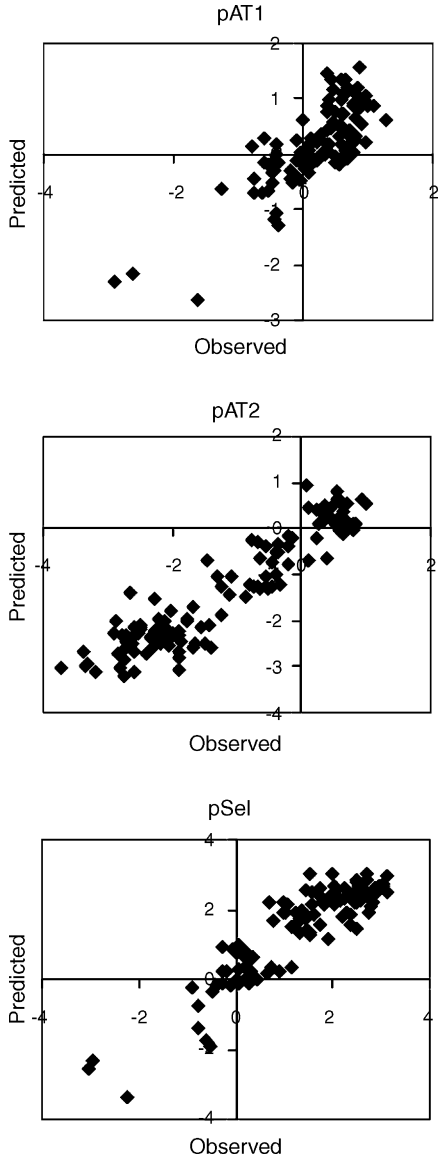

Fig. 4. Observed vs. predicted plots for each response (models 1, 2, and 3, respectively).

3.2. CoMFA modeling

In order to obtain a validated and predictive QSAR model we divided the data set into a training and test set [36], each consisting of 122 compounds (50% of the data set). The training set was selected based on the hierarchical clustering approach using the steric and electrostatic part of the CoMFA field as molecular descriptors and pAT1, pAT2 and pSel as response variables. The approach used to select training and test sets will certainly affect the outcome of the model statistics. For example, in our case, many of the generated clusters will only contain the compound that goes in to the training set while other clusters will contain both training and test set compounds. This will ensure that the compounds selected for the training set are diverse and representative of the whole data set. Models derived from such training sets will have a good chance to be generally predictive. However, the test set statistics may be overly optimistic since it is based on test set compounds that are always represented by a similar compound in the training set. Thus, these test set compounds will be relatively easy to predict as compared to a randomly selected test set [37] and this may lead to overoptimistic R^2_{pred} values. The opposite effect may be seen in the internal predictivity where diverse training sets might produce low Q^2 values. This will be the case when the model relies heavily on each data point during cross-validation when important compounds are excluded. Also, leaving a larger part of the data points out during cross-validation (i.e. leave-many-out) may produce low Q^2 as well.

The training set was used to derive the three separate models for pAT1, pAT2 and pSel (models 1, 2, and 3 in Table 1, respectively). All models have a Q^2 above 0.54 indicating that

Table 1
CoMFA models for pAT1, pAT2, and pSel

Response	Model no.	c[a]	R^2	Q^{2b}	SDEP	R^2_{pred}	R^2_{btsp}	S.D. R^2_{btsp}
pAT1	1	4	0.78	0.54	0.42	0.69	0.84	0.03
pAT2	2	3	0.82	0.69	0.51	0.86	0.85	0.03
pSel	3	5	0.89	0.69	0.57	0.80	0.93	0.02
pAT1	4[c]	4	0.79	0.56	0.66	0.59	–	–
pAT2	5[c]	4	0.92	0.86	0.66	0.79	–	–
pSel	6[c]	5	0.92	0.85	0.73	0.76	–	–

[a] Number of components.
[b] Crossvalidation using leave-20%-out.
[c] Models derived using switched training and test set.

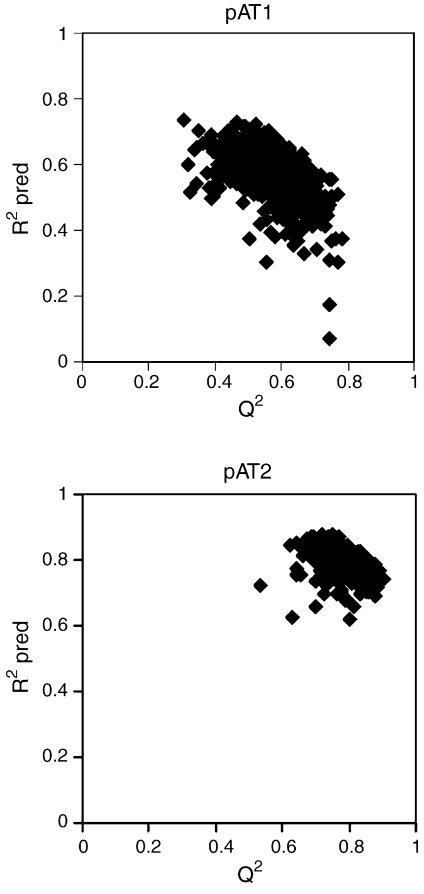

Fig. 5. Q^2 vs. R^2_{pred} for 1000 randomly assigned training and test sets.

they are internally predictive. The calculated R^2_{pred} values were also good, especially for the pAT2 and pSel response. Plots of predicted versus observed values for the responses can be seen in Fig. 4. To assess the potential of chance correlation, we also derived 100 models for each response using randomized y-data. The analysis showed that only five of the pAT1 models had a Q^2 between 0.0 and 0.1 while the rest of the pAT1 models had a negative Q^2. The models built using randomized pAT2- or pSel-data had even lower Q^2 values. This indicates that the good statistics obtained for the models based on the original data is not obtained by chance. The bootstrapping analysis (Table 1) also showed good results for all models (S.D. $R^2_{btsp} < 0.05$) [33].

To investigate the influence of the training set selection on the model statistics, models based on the compounds in the test set were derived and the training set compounds were used for prediction. These results are presented in Table 1 (models 4–6). In this case the resulting R^2_{pred} values were slightly lower and the Q^2 values were slightly higher for all the responses, which is consistent with the reasoning in the text above.

We believe that this approach of training set selection based on the response values and structural diversity, as defined by the CoMFA fields, is a good strategy for creating models with good predictivity. To illustrate this we generated 1000 random training sets (and test sets) for pAT1 and pAT2, respectively, and derived the corresponding CoMFA models. Plots of Q^2 versus R^2_{pred} for these models are shown in Fig. 5. Interestingly, for the pAT1 response only 15 models and for the pAT2 response only 11 models with better R^2_{pred} values were identified among the models based on a random training set. In contrast, 718 of the random models for the pAT1 response and 975 of the random models for the pAT2 response had better Q^2 values as compared to the model derived using the hierarchical design approach. This nicely illustrates the point discussed above that when a structurally diverse training set is used it is more difficult to obtain high Q^2 values. The inverse correlation between Q^2 and R^2_{pred} seen in Fig. 5 has also been noted by others [37].

Based on the CoMFA models 1, 2, and 3, contour plots were generated for pAT1, pAT2 and pSel (Fig. 6) in order to compare with the qualitative SAR and to obtain a general understanding of the QSAR. In the case of the selectivity analysis, the contour plots were illustrative for identifying features important for selectivity, an approach also used in other studies [38,39]. The contour plot of the AT_2 receptor affinity model (Fig. 6b) shows that there are many regions where increased steric bulk is

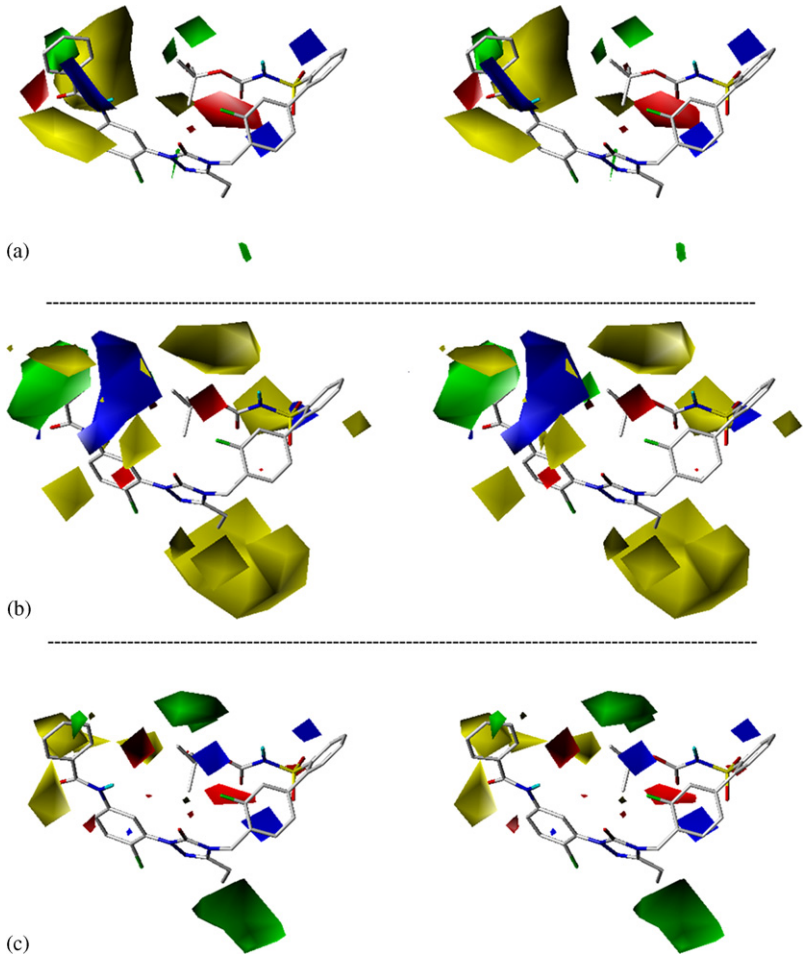

Fig. 6. Contour plots (upper 85th and lower 15th percentile for favorable and disfavorable interaction, respectively) in relaxed stereo view of CoMFA models for pAT1 (a), pAT2 (b) and pSel (c). Compound **1** is shown, with only essential hydrogen atoms displayed for clarity. Colored areas indicate features in the ligand correlated with higher affinity or higher AT_1 receptor selectivity (green = more steric bulk, yellow = less steric bulk, red = negative charge, blue = positive charge).

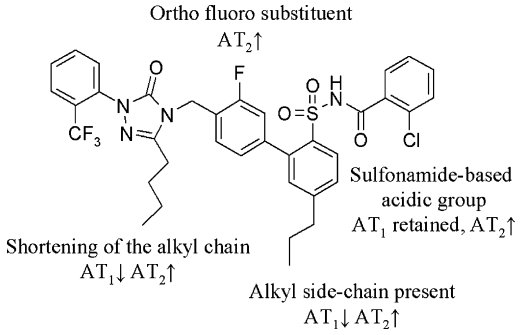

Fig. 7. Structural features important for AT_1 and AT_2 receptor affinity and selectivity.

associated with decreased affinity (yellow contours). Most of these regions are not seen in the model of AT_1 receptor affinity, which may indicate that the AT_2 receptor is more sensitive to steric bulk, at least for this data set. Many of the structural features that were found important for affinity and selectivity in the qualitative SAR [8,9] (some are shown in Fig. 7) are also seen in the contour plots. For example, replacing the tetrazole moiety found in losartan with a sulfonamide-based acidic group, in many cases resulted in an increased affinity for the AT_2 receptor while the AT_1 receptor affinity was retained. The different locations of the electrostatic contours (red and blue) in the pAT1 response model compared to pAT2, together with the sterically disfavored yellow contours in the pAT2 response model in the vicinity of the sulfonamide-based acidic group seem to support this observation. However, due to the large difference between a tetrazole and a sulfonamide-based acidic group, the latter with opportunities to provide an additional handle for substituents that further affects receptor affinity, the contours in this region are not trivial to rationalize. The contours originating from this sulfonamide side chain are different for the pAT1 and pAT2 models. In the pAT1 model a large yellow contour (sterically disfavored region) is located beyond the *t*-butyl group in **1** in Fig. 6a while this contour is absent in the pAT2 model (Fig. 6b). Furthermore, in the pAT2 model yellow contours align the side-chain, which are replaced by sterically favorable regions (green) in the pAT1 model. This indicates that short and bulky groups at this position are favorable for AT_1 receptor affinity while longer and less bulky groups seem to be favorable for AT_2 receptor affinity.

The *ortho*-fluoro substituent in the biphenyl moiety has been shown to enhance AT_2 receptor affinity, while in the case of AT_1 receptor affinity, the effect of this substituent has been more difficult to deduce. In a CoMFA study of AT_1 receptor ligands, structurally similar to the compounds in our data set, it was suggested that this *ortho*-fluoro substituent improved AT_1 receptor affinity [10]. However, in our analysis, the red contour close to the *ortho*-fluoro substituent (Fig. 6b) indicate that this is a favorable feature for AT_2 receptor affinity, while in the case of AT_1 receptor affinity, no interaction affecting the affinity can be observed in the contour plot at the selected levels. One reason for the difference observed between the models may be that different compounds were included in the modeling.

Comparison of the CoMFA maps in the area of the triazolinone/quinazolinone groups is also interesting. Shortening of the length of the *n*-butyl has been reported to decrease AT_1 receptor affinity and sometimes also increase AT_2 receptor affinity. This is nicely reflected by the green and yellow contours seen around this group in Fig. 6 for all responses. Furthermore in the region of the benzamide group in **1** (Fig. 6) there is a green contour present in both the pAT1 and pAT2 models showing that substituents in this region seem to be well-tolerated by both receptors. However, sterically disfavored regions are also present in this area suggesting that a well-defined shape of the substituents is necessary for optimal interactions (this has also been discussed in the case of AT_1 receptor affinity in another study [10]). Overall, the pAT1 and pAT2 models are similar in this region which is also reflected in the selectivity model (Fig. 6). In this model the contours are significantly reduced, indicating that this region is of less importance for determining AT_1/AT_2 receptor selectivity.

4. Conclusion

While many modeling studies of AT_1 receptor affinity have been published, there have been relatively few studies of AT_2 receptor affinity. Here we present highly predictive quantitative models developed using CoMFA on AT_1 and AT_2 receptor affinity as well as selectivity towards these receptors using a large number of compounds. The alignment and conformation of the compound classes was based on pharmacophore superimposition and the compounds used for building the models were selected using hierarchical clustering. The models have been validated using a test set, also obtained from the hierarchical clustering. We aim to use these models for future guidance and development of in-house angiotensin II receptor ligands as an ongoing project in our department [40,41].

Acknowledgments

We gratefully acknowledge support from the Swedish Foundation for Strategic Research. We thank Henrik Karlsson for assistance in collecting literature data and preliminary CoMFA calculations.

Appendix A. Supplementary data

Supplementary data associated with this article can be found, in the online version, at doi:10.1016/j.jmgm.2006.10.004.

List of compounds used in modeling, the training and test set as 3D structure files in mol2 format, and a figure showing the reduced set of comparison atoms used in the conformational analysis are available as supplementary material.

References

[1] M. de Gasparo, K.J. Catt, T. Inagami, J.W. Wright, T. Unger, International union of pharmacology. XXIII. The angiotensin II receptors, Pharmacol. Rev. 52 (2000) 415–472.

[2] M. Stoll, T. Unger, Angiotensin and its AT2 receptor: new insights into an old system, Regul. Pept. 99 (2001) 175–182.
[3] E. Kaschina, T. Unger, Angiotensin AT1/AT2 receptors: regulation, signalling and function, Blood Pressure 12 (2003) 70–88.
[4] B. Johansson, M. Holm, S. Ewert, A. Casselbrant, A. Pettersson, L. Fandriks, Angiotensin II type 2 receptor-mediated duodenal mucosal alkaline secretion in the rat, Am. J. Physiol. 280 (2001) G1254–G1260.
[5] R.M. Carey, Angiotensin type-2 receptors and cardiovascular function: are angiotensin type-2 receptors protective? Curr. Opin. Cardiol. 20 (2005) 264–269.
[6] R.E. Widdop, E.S. Jones, R.E. Hannan, T.A. Gaspari, Angiotensin AT2 receptors: cardiovascular hope or hype? Br. J. Pharmacol. 140 (2003) 809–824.
[7] U.M. Steckelings, E. Kaschina, T. Unger, The AT2 receptor-A matter of love and hate, Peptides 26 (2005) 1401–1409.
[8] L.L. Chang, W.J. Greenlee, Angiotensin II receptor antagonists: nonpeptides with equivalent high affinity for both the AT1 and AT2 subtypes, Curr. Pharm. Design 1 (1995) 407–424.
[9] W.T. Ashton, L.L. Chang, K.L. Flanagan, N.B. Mantlo, D.L. Ondeyka, D. Kim, S.E. de Laszlo, T.W. Glinka, R.A. Rivero, N.J. Kevin, R.S.L. Chang, P.K.S. Siegl, S.D. Kivlighn, W.J. Greenlee, AT1/AT2-balanced angiotensin II antagonists, Eur. J. Med. Chem. 30 (1995) 255–266.
[10] P. Datar, P. Desai, E. Coutinho, K. Iyer, CoMFA and CoMSIA studies of angiotensin (AT1) receptor antagonists, J. Mol. Model. 8 (2002) 290–301.
[11] T. Pandya, S.K. Pandey, M. Tiwari, S.C. Chaturvedi, A.K. Saxena, 3-D QSAR studies of triazolinone based balanced AT1/AT2 receptor antagonists, Bioorg. Med. Chem. 9 (2001) 291–300.
[12] T. Pandya, S.C. Chaturvedi, Structure–activity relationship study of some triazolinone based compounds with antagonistic balanced activity on angiotensin II receptor subtypes AT1 and AT2. A three-dimensional quantitative structure-activity relationship investigation, Arzneimittel-Forsch. 55 (2005) 265–270.
[13] G. Berellini, G. Cruciani, R. Mannhold, Pharmacophore Drug Metabolism, and Pharmacokinetics Models on Non-Peptide AT1, AT2, and AT1/AT2 Angiotensin II Receptor Antagonists, J. Med. Chem. 48 (2005) 4389–4399.
[14] L. Belvisi, G. Bravi, G. Catalano, M. Mabilia, A. Salimbeni, C. Scolastico, A 3D QSAR CoMFA study of non-peptide angiotensin II receptor antagonists, J. Comput. Aid. Mol. Des. 10 (1996) 567–582.
[15] S.E. de Laszlo, T.W. Glinka, W.J. Greenlee, R. Ball, R.B. Nachbar, K. Prendergast, The design, binding affinity prediction and synthesis of macrocyclic angiotensin II AT1 and AT2 receptor antagonists, Bioorg. Med. Chem. Lett. 6 (1996) 923–928.
[16] Y.C. Martin, M.G. Bures, E.A. Danaher, J. DeLazzer, I. Lico, P.A. Pavlik, A fast new approach to pharmacophore mapping and its application to dopaminergic and benzodiazepine agonists, J. Comput. Aid. Mol. Des. 7 (1993) 83–102.
[17] R.D. Cramer III, D.E. Patterson, J.D. Bunce, Comparative molecular field analysis (CoMFA). 1. Effect of shape on binding of steroids to carrier proteins, J. Am. Chem. Soc. 110 (1988) 5959–5967.
[18] T.W. Glinka, S.E. de Laszlo, J. Tran, R.S. Chang, T.B. Chen, V.J. Lotti, W.J. Greenlee, L-161, 638: a potent AT2 selective quinazolinone angiotensin II binding inhibitor, Bioorg. Med. Chem. Lett. 4 (1994) 1479–1484.
[19] S.E. de Laszlo, C.S. Quagliato, W.J. Greenlee, A.A. Patchett, R.S.L. Chang, V.J. Lotti, T.B. Chen, S.A. Scheck, K.A. Faust, S.S. Kivlighn, T.S. Schorn, G.J. Zingaro, P.K.S. Siegl, A potent, orally active, balanced affinity angiotensin II AT1 antagonist and AT2 binding inhibitor, J. Med. Chem. 36 (1993) 3207–3210.
[20] T.W. Glinka, S.E. de Laszlo, P.K.S. Siegl, R.S. Chang, S.D. Kivlighn, T.S. Schorn, K.A. Faust, T.-B. Chen, G.J. Zingaro, V.J. Lotti, W.J. Greenlee, A new class of balanced AT1/AT2 angiotensin II antagonists: quinazolinone AII antagonists with acylsulfonamide and sulfonylcarbamate acidic functionalities, Bioorg. Med. Chem. Lett. 4 (1994) 81–86.
[21] P.K. Chakravarty, R.A. Strelitz, T.B. Chen, R.S.L. Chang, V.J. Lotti, G.J. Zingaro, T.W. Schorn, S.D. Kivlighn, P.K.S. Siegl, A.A. Patchett, W.J. Greenlee, Quinazolinone biphenyl acylsulfonamides: a potent new class of angiotensin-II receptor antagonists, Bioorg. Med. Chem. Lett. 4 (1994) 75–80.
[22] L.L. Chang, W.T. Ashton, K.L. Flanagan, T.-B. Chen, S.S. O'Malley, G.J. Zingaro, P.K.S. Siegl, S.D. Kivlighn, V.J. Lotti, R.S.L. Chang, W.J. Greenlee, Triazolinone biphenylsulfonamides as angiotensin II receptor antagonists with high affinity for both the AT1 and AT2 subtypes, J. Med. Chem. 37 (1994) 4464–4478.
[23] L.L. Chang, W.T. Ashton, K.L. Flanagan, R.A. Rivero, T.B. Chen, S.S. O'Malley, G.J. Zingaro, S.D. Kivlighn, P.K.S. Siegl, V.J. Lotti, R.S.L. Chang, W.J. Greenlee, Potent triazolinone-based angiotensin II receptor antagonists with equivalent affinity for both the AT1 and AT2 subtypes, Bioorg. Med. Chem. Lett. 4 (1994) 2787–2792.
[24] L.L. Chang, W.T. Ashton, K.L. Flanagan, T.-B. Chen, S.S. O'Malley, G.J. Zingaro, S.D. Kivlighn, P.K.S. Siegl, V.J. Lotti, R.S.L. Chang, W.J. Greenlee, Potent and orally active angiotensin II receptor antagonists with equal affinity for human AT1 and AT2 subtypes, J. Med. Chem. 38 (1995) 3741–3758.
[25] W.T. Ashton, L.L. Chang, K.L. Flanagan, S.M. Hutchins, E.M. Naylor, P.K. Chakravarty, A.A. Patchett, W.J. Greenlee, T.-B. Chen, K.A. Faust, R.S.L. Chang, V.J. Lotti, G.J. Zingaro, T.W. Schorn, P.K.S. Siegl, S.D. Kivlighn, Triazolinone biphenylsulfonamide derivatives as orally active angiotensin II antagonists with potent AT1 receptor affinity and enhanced AT2 affinity, J. Med. Chem. 37 (1994) 2808–2824.
[26] F. Mohamadi, N.G.J. Richards, W.C. Guida, R. Liskamp, M. Lipton, C. Caufield, G. Chang, T. Hendrickson, W.C. Still, MacroModel—an integrated software system for modeling organic and bioorganic molecules using molecular mechanics, J. Comput. Chem. 11 (1990) 440–467.
[27] J.M. Goodman, W.C. Still, An unbounded systematic search of conformational space, J. Comput. Chem. 12 (1991) 1110–1117.
[28] J.W. Ponder, F.M. Richards, An efficient Newton-like method for molecular mechanics energy minimization of large molecules, J. Comput. Chem. 8 (1987) 1016–1024.
[29] W.C. Still, A. Tempczyk, R.C. Hawley, T. Hendrickson, Semianalytical treatment of solvation for molecular mechanics and dynamics, J. Am. Chem. Soc. 112 (1990) 6127–6129.
[30] Sybyl, version 6.9 and 7.1, Tripos, Inc., St. Louis, MO.
[31] M.J.S. Dewar, E.G. Zoebisch, E.F. Healy, J.J.P. Stewart, Development and use of quantum mechanical molecular models. 76. AM1: a new general purpose quantum mechanical molecular model, J. Am. Chem. Soc. 107 (1985) 3902–3909.
[32] K.H. Kim, G. Greco, E. Novellino, A critical review of recent CoMFA applications, Perspect. Drug Discov. 12–14 (1998) 257–315.
[33] R.D. Cramer III, J.D. Bunce, D.E. Patterson, I.E. Frank, Crossvalidation, bootstrapping, and partial least squares compared with multiple regression in conventional QSAR studies, Quant. Struct. Acta Relat. 7 (1988) 18–25.
[34] S.D. Peterson, W. Schaal, A. Karlen, Improved CoMFA modeling by optimization of settings, J. Chem. Inf. Model. 46 (2006) 355–364.
[35] F.H. Allen, The Cambridge structural database: a quarter of a million crystal structures and rising., Acta Crystallogr. Sect. B: Struct. Sci. B 58 (2002) 380–388.
[36] A. Golbraikh, M. Shen, Z. Xiao, Y.-D. Xiao, K.-H. Lee, A. Tropsha, Rational selection of training and test sets for the development of validated QSAR models, J. Comput. Aid. Mol. Des. 17 (2003) 241–253.
[37] R.D. Clark, Boosted leave-many-out cross-validation: the effect of training and test set diversity on PLS statistics, J. Comput. Aid. Mol. Des. 17 (2003) 265–275.
[38] I.I. Baskin, I.G. Tikhonova, V.A. Palyulin, N.S. Zefirov, Selectivity fields: comparative molecular field analysis (CoMFA) of the glycine/NMDA and AMPA receptors, J. Med. Chem. 46 (2003) 4063–4069.
[39] G. Wong, K.F. Koehler, P. Skolnick, Z.Q. Gu, S. Ananthan, P. Schonholzer, W. Hunkeler, W. Zhang, J.M. Cook, Synthetic and computer-assisted analysis of the structural requirements for selective, high-affinity ligand binding to diazepam-insensitive benzodiazepine receptors, J. Med. Chem. 36 (1993) 1820–1830.
[40] Y. Wan, C. Wallinder, B. Johansson, M. Holm, A.K. Mahalingam, X. Wu, M. Botros, A. Karlen, A. Pettersson, F. Nyberg, L. Faendriks, A. Hallberg, M. Alterman, First reported nonpeptide AT1 receptor agonist (L-162,313)

acts as an AT2 receptor agonist in vivo, J. Med. Chem. 47 (2004) 1536–1546.
[41] Y. Wan, C. Wallinder, B. Plouffe, H. Beaudry, A.K. Mahalingam, X. Wu, B. Johansson, M. Holm, M. Botoros, A. Karlen, A. Pettersson, F. Nyberg, L. Faendriks, N. Gallo-Payet, A. Hallberg, M. Alterman, Design, synthesis, and biological evaluation of the first selective nonpeptide AT2 receptor agonist, J. Med. Chem. 47 (2004) 5995–6008.